© 2016. Published by The Company of Biologists Ltd | Journal of Cell Science (2016) 129, 1722-1733 doi:10.1242/jcs.181545

RESEARCH ARTICLE

The GATA transcription factor gene *gtaG* is required for terminal differentiation in *Dictyostelium*

Mariko Katoh-Kurasawa*, Balaji Santhanam and Gad Shaulsky*

ABSTRACT

The GATA transcription factor GtaG is conserved in Dictyostelids and is essential for terminal differentiation in *Dictyostelium discoideum*, but its function is not well understood. Here, we show that *gtaG* is expressed in prestalk cells at the anterior region of fingers and in the extending stalk during culmination. The *gtaG*$^{-}$ phenotype is cell-autonomous in prestalk cells and non-cell-autonomous in prespore cells. Transcriptome analyses reveal that GtaG regulates prestalk gene expression during cell differentiation before culmination and is required for progression into culmination. GtaG-dependent genes include genetic suppressors of the Dd-STATa-defective phenotype (Dd-STATa is also known as DstA) as well as Dd-STATa target-genes, including extracellular matrix genes. We show that GtaG might be involved in the production of two culmination-signaling molecules, cyclic di-GMP (c-di-GMP) and the spore differentiation factor SDF-1, and that addition of c-di-GMP rescues the *gtaG*$^{-}$ culmination and spore formation deficiencies. We propose that GtaG is a regulator of terminal differentiation that functions in concert with Dd-STATa and controls culmination through regulating c-di-GMP and SDF-1 production in prestalk cells.

KEY WORDS: GtaG, *Dictyostelium*, Terminal differentiation, c-di-GMP, SDF-1

INTRODUCTION

Dictyostelium discoideum is a free-living soil amoeba. Individual cells prey on bacteria and divide as solitary amoebae when food is abundant. In the laboratory, they grow in association with bacteria or axenically in defined liquid medium. When the amoebae starve, they stop dividing and begin to aggregate, forming multicellular structures of about 100,000 cells each. The multicellular organisms begin to develop and undergo a series of morphological changes. After initial formation of loose aggregates at around 8–10 h of development, the structures envelope themselves in a cellulosic sheath and become tight aggregates at about 12 h. During that time, the cells differentiate into prestalk (about 30% of the population) and prespore cells (about 70%) that are initially intermixed. Later, the prespore and prestalk cells segregate from one another. Most of the prestalk cells migrate to the top of the tight aggregate, forming a tip that leads the elongation of the structure until it assumes a finger shape. At that stage, about 16 h into development, the anterior part of the structure comprises solely prestalk cells, and the posterior contains mostly prespore cells and a small proportion of prestalk cells. The prestalk cells at the very tip of the finger are called prestalk A (PST-A) cells, and the prestalk cells immediately behind them are called prestalk O (PST-O) cells. The cells in the posterior part of the prestalk region near the substratum are called prestalk B (PST-B) cells. The prestalk cells that are scattered throughout the posterior part of the finger are called anterior-like cells (ALCs). In certain instances, the fingers might fall over and migrate on the substrate as slugs, which utilize phototaxis and thermotaxis to reach the surface of the soil. The final stages of development begin as the slugs erect themselves into a second finger. The bottom of the finger expands and shortens until the structure assumes a 'Mexican hat' shape. At that stage, the prestalk cells at the top of the structure begin to accumulate a large internal water vacuole and deposit a cellulosic cell wall around themselves. As they do so, they descend through the prespore cell mass while forming a stalk tube. Once the elongating stalk tube hits the substratum, the entire structure begins to rise away from the surface along the stalk tube in a process called culmination. During that time, the prespore cells begin to sporulate – they become desiccated and enveloped in a thick spore coat. The final fruiting body comprises a cellular stalk, about 1 mm tall, that carries a ball (sorus) full of spores. The spores can disperse and germinate when food is abundant again, whereas the stalk cells die in place. The entire developmental process takes about 24 h and it is highly synchronous, such that thousands of aggregates develop and undergo morphogenesis in lockstep (Kessin, 2001).

The developmental process is accompanied by differentiation at various levels, including gene expression. Examination of the developmental transcriptome has revealed vast changes in gene expression that occur in bursts during different developmental stages (Rosengarten et al., 2015). The most prominent change in gene expression coincides with the transition from unicellularity to multicellularity, at around 8–10 h of development. Initial changes take place in most cells, but differentiation into prespore and prestalk cells is accompanied by expression of cell-type-specific genes (Parikh et al., 2010). The pattern of cell-type-specific gene expression, as studied by performing *in situ* RNA hybridization, has been used to define several subsets of prespore and prestalk domains in the finger and to reveal specific markers for these subtypes (Maeda et al., 2003). Patterns that have been determined with *in situ* RNA hybridization largely agree with patterns of gene expression that have been studied by using reporter gene fusions (e.g. GFP or *lacZ*) and by performing RNA-seq analyses of separated cell types (Parikh et al., 2010), suggesting that most of the transcriptome dynamics is determined by regulating promoter activity.

One of the intriguing properties of *Dictyostelium* development is the striking similarity between the developmental transcriptomes of *D. discoideum* and *D. purpureum* (Kessin, 2010). These two species are as evolutionarily diverged as humans and fish (Sucgang et al., 2011), yet their developmental transcriptomes are nearly 50% identical (Parikh et al., 2010). It is therefore interesting to explore the conserved mechanisms that regulate these transcriptomes.

The *D. discoideum* genome is surprisingly poor in genes that encode transcription factors (Eichinger et al., 2005). In fact, it has

Department of Molecular and Human Genetics, Baylor College of Medicine, One Baylor Plaza, Houston, TX 77030, USA.

*Authors for correspondence (mkatoh@bcm.edu; gadi@bcm.edu)

Received 1 October 2015; Accepted 20 February 2016

Journal of Cell Science (2016) 129, 1722-1733 doi:10.1242/jcs.181545

the lowest fraction of genes that encode transcription factors among all known eukaryotic genomes (Shaulsky and Huang, 2005). Some of the transcription factors have been studied in detail, and they appear to have a wide range of roles in development (Schnitzler et al., 1994; Chang et al., 1996; Escalante and Sastre, 1998; Mu et al., 2001; Thompson et al., 2004; Huang et al., 2006, 2011; Cai et al., 2014). One of the most recently described transcription factors is *gtaC*, which is a central regulator of gene expression during aggregation and in subsequent developmental stages (Keller and Thompson, 2008; Cai et al., 2014; Santhanam et al., 2015). Examination of several transcription factors, including *stkA*, *gtaC*, *srfA* and *gbfA*, suggests that conservation of sequence and expression patterns between *D. discoideum* and *D. purpureum* is tightly correlated with key regulatory functions in development (Rosengarten et al., 2013). We are using this guideline in our quest to analyze the transcriptional regulators of the *D. discoideum* developmental process.

In this report, we analyzed the role of *gtaG* in development. We found that *gtaG* expression and amino acid sequence are conserved in various Dictystelids and that *gtaG* activity is essential for prestalk development in a cell-autonomous manner. Transcriptional analysis revealed that *gtaG* is involved in the regulation of prestalk gene expression and that its activity overlaps with that of another well-characterized transcription factor, Dd-STATa (also known as DstA). *gtaG* appears to be directly involved in terminal prestalk differentiation, and indirectly involved in culmination and sporulation. Both activities appear to be mediated by regulation of cyclic di-GMP (c-di-GMP) and Spore Differentiation Factor-1 (SDF-1) production.

RESULTS

gtaG is evolutionarily conserved and enriched in the prestalk

gtaG is an intronless gene that encodes a GATA transcription factor on the Crick strand of *D. discoideum* Chromosome 1. The open reading frame (ORF) length is 3018 bp, and the predicted protein contains 1006 amino acid residues with a calculated molecular weight of 110.9 kDa, according to dictyBase (Basu et al., 2015). The protein sequence includes a nuclear localization signal (NLS) and a single conserved $CX_2CX_{18}CX_2C$ motif (where X represents any amino acid) that is characteristic of non-vertebrate zinc-finger proteins type IVb (Teakle and Gilmartin, 1998; Lowry and Atchley, 2000), followed by a short basic domain. The predicted protein sequence is highly conserved in *D. purpureum*, *Polysphondylium pallidum* and *D. fasciculatum* (Fig. S1A). Comparing the gene expression profiles of *gtaG* in the developmental time courses of *D. discoideum* and *D. purpureum* (Parikh et al., 2010) indicates that the two organisms have similar *gtaG* mRNA abundance profiles. In both organisms, *gtaG* mRNA is developmentally regulated, with almost no expression at the onset of development and increasing accumulation thereafter (Fig. S1B). The mRNA is preferentially expressed in prestalk cells in both organisms (Fig. S1C). This conservation of coding sequences and gene regulation suggests conservation of function.

gtaG is expressed in prestalk cells and required for terminal differentiation

A restriction-enzyme-mediated integration (REMI) mutation in the *gtaG* gene leads to developmental arrest at the slug stage in development on non-nutrient agar (mutant V10633, described in Sawai et al., 2007). We recapitulated the REMI mutation (Fig. S2) and studied the phenotype in more detail. We found that development of the *gtaG*$^-$ cells was morphologically indistinguishable from wild-type development up to 12 h (Fig. 1A). We started to observe slight differences at 16 h, when both strains formed fingers; the mutant fingers were slightly more plump and shorter than the wild-type fingers. The differences became even more pronounced in the following 8 h – the wild type continued to develop into early culminants at 20 h and fruiting bodies, comprising stalks and sori, at 24 h, whereas most of the mutant structures remained at the finger stage (Fig. 1A). We also observed a few feeble fruiting bodies at 24 h of *gtaG*$^-$ development. These differences were also observed in cells that had been grown on nutrient agar plates in association with bacteria. Both mutant and wild-type strains made plaques in the bacterial lawn, and both developed multicellular structures inside the plaque, but the *gtaG*$^-$ cells formed aberrant structures that resembled slugs with a curly trail behind them, whereas the wild type formed proper fruiting bodies (Fig. 1B). The absence of slime trails around the *gtaG*$^-$ plaque suggests the mutant is not a 'slugger' (Fukuzawa et al., 1997) (Fig. 1B).

We verified the insertional mutation in *gtaG* by performing Southern blot and PCR analysis (Fig. S2), but we were unsure whether the insertion had generated a null allele. We therefore tested *gtaG* mRNA expression in the wild type and in the mutant using RNA-seq. Fig. S2D shows that the *gtaG* mRNA was truncated at the REMI plasmid insertion site, and Fig. S2D and E show that the region encoding the zinc-finger domain was not transcribed during development of the *gtaG*$^-$ mutant cells. Nevertheless, it is possible that the *gtaG* mRNA upstream of the insertion site has a function that could account for the phenotype. We therefore generated a deletion allele of *gtaG* by replacing most of the coding domain, including the NLS, with a Blasticidin-S-resistance cassette (BSR), such that the region downstream of the replacement was out of frame and not transcribed (Fig. S3A). We validated the gene replacement by performing Southern blot and PCR analysis (Fig. S3B,C). The phenotype conferred by the deletion allele was indistinguishable from the phenotype conferred by the *gtaG*$^-$ REMI insertion – normal development up to the finger stage and developmental arrest thereafter (Fig. S3D). These results suggest that both alleles cause a loss of *gtaG* function. Subsequent experiments were performed using the REMI insertion mutation.

The developmental defects we observed suggest that both spore and stalk differentiation are compromised in the mutant, but according to RNA-seq analysis (Parikh et al., 2010), *gtaG* expression is highly enriched in prestalk cells (Fig. S1C). In order to validate the prestalk enrichment of *gtaG* expression, we generated a reporter construct by fusing the *gtaG* promoter to the *Escherichia coli lacZ* gene. X-gal staining of wild-type cells that had been transformed with the *gtaG/lacZ* reporter indicated promoter activity in PST-A cells, at the very tip of the prestalk region of fingers (Fig. 1C) and very weak staining in some of the ALC population after staining for a long time with X-gal (data not shown). Stained cells were also evident in the elongating stalk tube at early culmination and throughout the stalk at late culmination. These results confirm the observation that *gtaG* is expressed exclusively in PST-A and stalk cells, suggesting that the sporulation defect in the *gtaG*$^-$ mutant is non-cell-autonomous.

To test that possibility directly, we performed mixing experiments between wild-type and *gtaG*$^-$ mutant cells (Fig. 1D). Development of pure populations confirmed that the *gtaG*$^-$ mutant cells had a sporulation defect – their sporulation efficiency was about one-quarter of that of the wild type. Mixing the *gtaG*$^-$ mutant cells with an equal number of wild-type cells restored the mutant sporulation efficiency to near wild-type levels without

Journal of Cell Science (2016) 129, 1722-1733 doi:10.1242/jcs.181545

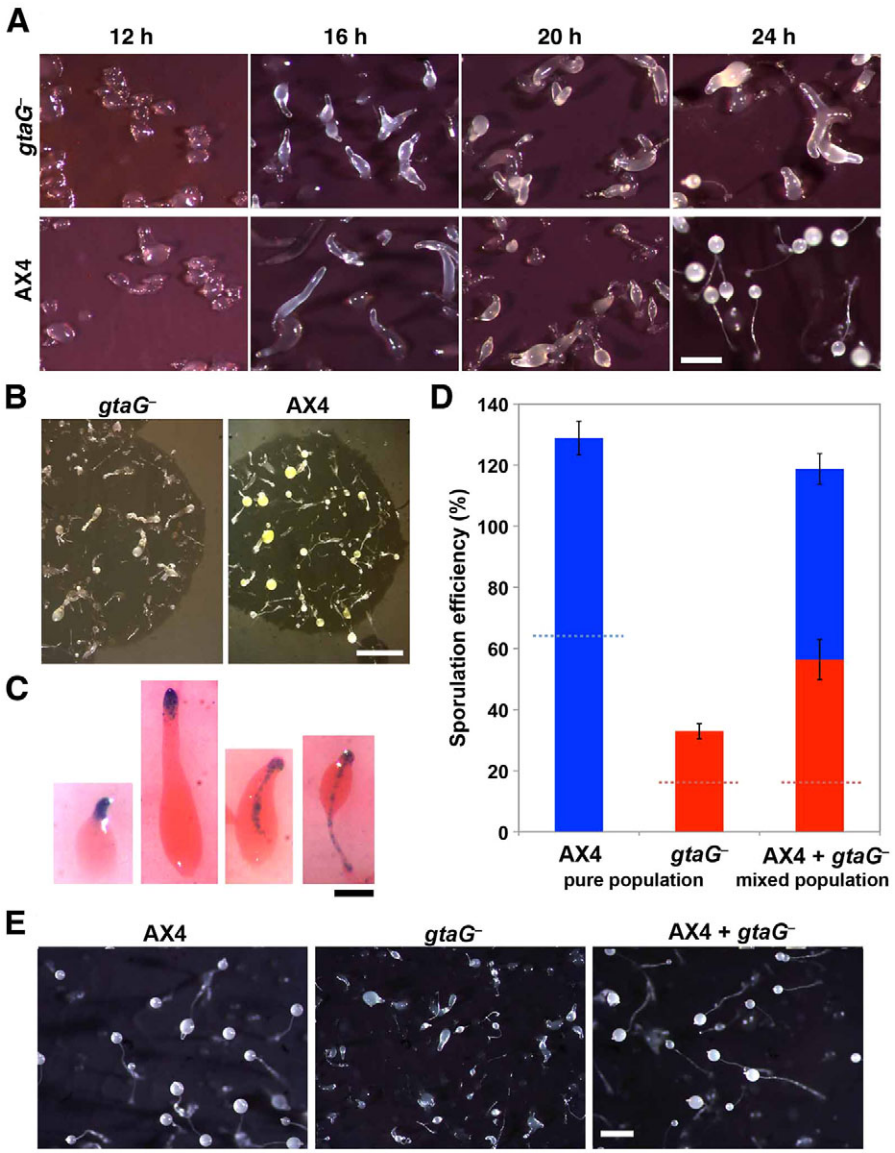

Fig. 1. The *gtaG*⁻ gene is required for terminal development. (A) We developed the *gtaG*⁻ mutant (top) and the wild type (AX4, bottom) on black nitrocellulose filters, and photographed the multicellular structures at 12, 16, 20 and 24 h, as indicated above the panels. Scale bar: 0.5 mm. (B) We grew *gtaG*⁻ mutant and wild-type (AX4) cells on bacterial lawns, and photographed a single plaque of each 3 days after the cells had started to aggregate in the plaques. The dim ocher surface at the right side of the picture is the lawn of intact bacteria. The darker partial circle at the center of the picture is the plaque where the amoebae ate the bacteria. The white-tinged forms emerging from the plaque are the developing multicellular structures. Scale bar: 2.0 mm. (C) We generated a reporter construct in which the *gtaG* promoter was fused with the *E. coli lacZ* gene. We transformed wild-type cells with the reporter and visualized promoter *gtaG* activity by performing X-gal staining (blue) followed by counterstaining with eosin Y (red). Representative pictures show a tipped mound (14 h, left panel), a finger (16 h, second left panel), an early culminant (18 h, second right panel) and a mid-culminant (20 h, right panel). Scale bar: 0.2 mm. (D) We measured the sporulation of a GFP-tagged *gtaG*⁻ mutant strain and the wild type (AX4) in pure populations and in a 1:1 mixed population, as indicated, after 40 h of development on filters. The sporulation efficiency (%, y-axis) of each strain was expressed as the fraction of spores relative to the number of cells plated for development. In the stacked bars, red represents the *gtaG*⁻ mutant and blue represents the wild type (AX4). The spore genotypes were distinguished by their GFP fluorescence using flow cytometry. The data are the means±s.e.m. of 11 replicates. Dashed lines show half levels of sporulation efficiency in each pure population and the levels expected in the absence of synergy in the mixed population. (E) Terminal developmental morphologies (40 h) of cells that had been developed on dark filters as above: pure populations of *gtaG*⁻ mutant and the wild type (AX4), and a 1:1 mixed population as indicated above each panel. Scale bar: 0.5 mm.

compromising the sporulation efficiency of the wild type. These results suggest that *gtaG*⁻ confers a non-cell-autonomous defect on sporulation. Developmental morphogenesis also appeared to be restored in the mixed population (Fig. 1E).

Transcriptome analysis of *gtaG*⁻ cells

We analyzed the transcriptomes of *gtaG*⁻ and wild-type cells as a means of comparing their molecular phenotypes (GEO accession number: GSE70558). Transcriptome-wide gene expression comparisons can be summarized by multi-dimensional scaling (MDS) (Santhanam et al., 2015). Briefly, the transcriptome of each strain can be thought of as a single point in a multidimensional space, where each gene defines a dimension and each mRNA abundance value determines the position of the point in that dimension. An MDS plot provides a two-dimensional view that is the best representation of the multidimensional distances between the points. When two points in the graph are close, it means that the transcriptomes of the two samples are similar to one another. Fig. 2A compares the transcriptional phenotypes of the wild type and the *gtaG*⁻ mutant. At early stages of development, the transcriptomes of the two strains are nearly indistinguishable – there is almost no distance between the *gtaG*⁻ and the wild-type points at 0–8 h. It is also noticeable that the 0-h and 4-h samples cluster together, and there is a big distance between them and the 8-h sample, consistent with the finding that the biggest transcriptional transition in *D. discoideum* development occurs during the transition from single cells to multicellular behavior (Van Driessche et al., 2002; Parikh et al., 2010; Rosengarten et al., 2015). The distances between the two strains at 12 and 16 h are also rather small. These findings, which rely on the mRNA abundance of all the genes in the genome, are consistent with the more subjective morphological comparison (Fig. 1A). Examination of the last two time points reveals that although the wild-type transcriptome continued to progress at 20 h and 24 h, the *gtaG*⁻ transcriptome remained rather similar to the 16-h transcriptome at those time points (Fig. 2A). This finding is consistent with the lack of morphological progression beyond the finger stage (Fig. 1). These findings suggest that the morphological arrest of *gtaG*⁻ at the finger stage is the result of attenuation in the overall developmental program of the mutant cells.

Comparing the transcriptome of the wild type to that of a transcription-factor-defective mutant is a way of identifying

Journal of Cell Science (2016) 129, 1722-1733 doi:10.1242/jcs.181545

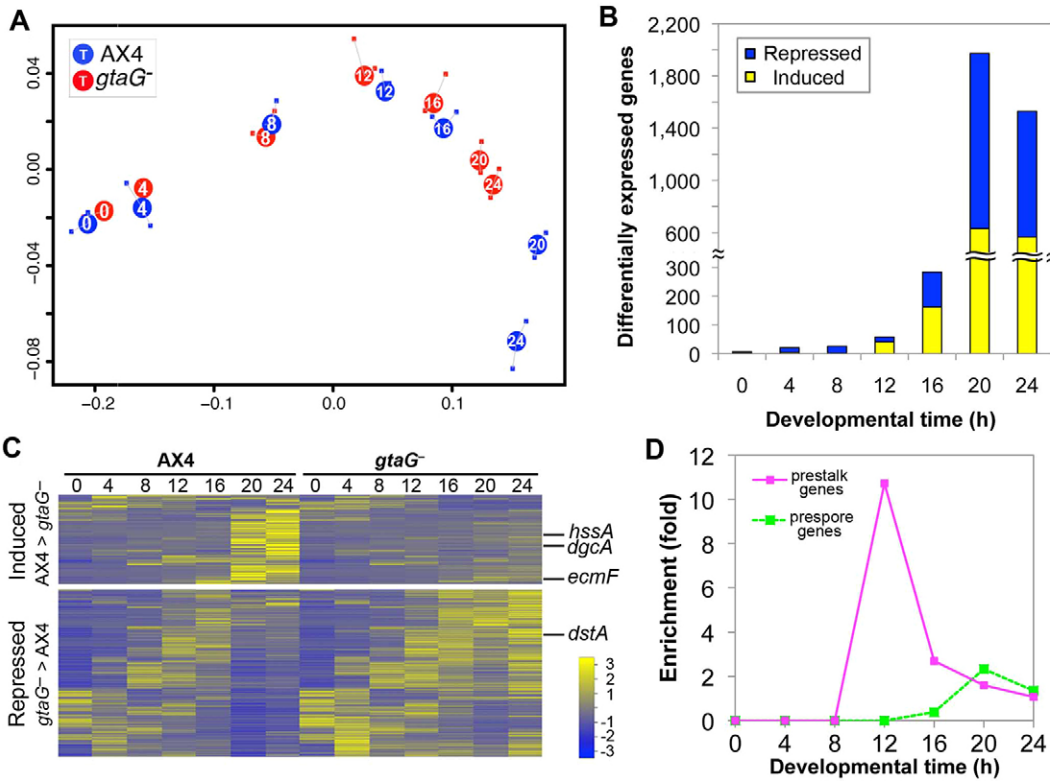

Fig. 2. Transcriptome differences between *gtaG*⁻ and the wild type. We developed cells on nitrocellulose filters for 24 h and analyzed samples by performing RNA-seq at 4-h intervals. (A) Multi-dimensional scaling (MDS) visualization of distances between the transcriptomes of the *gtaG*⁻ mutant (red) and the wild type AX4 (blue). Each circle represents the average of two independent biological replicates, which are represented as small squares and whiskers (in some cases, the squares are covered by the circles). Numbers inside the circles indicate the developmental time (hours). The axes units are arbitrary. (B) The number of differentially expressed genes between *gtaG*⁻ and AX4 (y-axis) as a function of developmental time (x-axis, hours). Yellow, GtaG-induced genes (mRNA abundance in AX4 is significantly greater than mRNA abundance in *gtaG*⁻); blue, GtaG-repressed genes (mRNA abundance in AX4 is significantly lower than mRNA abundance in *gtaG*⁻). Notice that the y-axis is split to show details in the early time points. (C) The heat map shows the change in standardized mRNA abundances of genes that were differentially expressed between *gtaG*⁻ and AX4 cells, as indicated on the left, during the entire developmental process. Strain names and developmental time points (hours) are indicated above the columns. Each row represents a gene, and the colors represent relative mRNA abundances (see scale). Selected gene names are indicated on the right. (D) Enrichment of prespore-specific genes (green) and prestalk-specific genes (magenta) among the differentially expressed genes (y-axis) as a function of developmental time (x-axis, hours).

potential transcriptional targets for that factor (Cai et al., 2014). We performed differential expression analysis at each time point and found over 3000 genes that exhibited differential expression between the wild type and the *gtaG*⁻ mutant throughout development (Tables S1A, S2). Fig. 2B shows the number of differentially expressed genes as a function of developmental time, indicating that the maximal level of differential expression is seen at 20 h of development. This result is also consistent with the lack of further developmental progression in the mutant (Fig. 1). The 1071 genes whose expression is higher in the wild type than in the mutant at any one of the time points are potential activated targets of GtaG (induced), and the 2009 genes whose expression is lower in the wild type are potential repressed targets (repressed) (Fig. 2C). The GO-enrichment analysis of these two gene sets is presented in Table 1. In the induced-gene list, the terms ‘cellulose binding’ and ‘extracellular region’ suggest roles in extracellular matrix production. The terms ‘sporulation’ and ‘cell differentiation’ are consistent with the developmental defects and the non-cell-autonomous nature of the sporulation phenotype, and the term ‘cell morphogenesis’ is consistent with the overall morphological and developmental arrest. In the repressed gene list, the terms ‘gene silencing’, ‘histone deacetylation’ and ‘core TFIIH complex’ are enriched, suggesting that there is a general transcriptional response.

GtaG is a putative transcription factor that functions in the latter half of development, so we were mainly interested in GtaG-induced genes that were differentially expressed at late stages of development. We also explored the cell-type preference of GtaG-induced genes because *gtaG* itself is preferentially expressed in prestalk cells. We found that prestalk genes were significantly overrepresented among GtaG-induced genes at 12 and 16 h of development (Fig. 2D; Table S1B), supporting the idea that GtaG is a prestalk-specific transcription factor. Interestingly, however, prespore genes were more enriched at 20 h of development (Fig. 2D; Table S1B). Considering the expression levels of *gtaG* itself and the phenotypes of the *gtaG*⁻ mutant, we closely looked at early GtaG-induced genes in 12- and 16-h samples (Table S2). At 12-h and 16-h of development, 41 and 163 genes, respectively, are induced by GtaG (Table S1A), and both sets include two types of gene families that encode hssA/2C/7E-family proteins and uncharacterized 57-amino-acid proteins (Table S1B). The *hssA* gene, which encodes a 93-amino-acid polypeptide, was originally identified as a high-copy suppressor of the Dd-STATa mutant. However, its expression is independent of Dd-STATa and dependent on GbfA (Iranfar et al., 2006; Shimada et al., 2008). Dd-STATa was overexpressed after 12 h of development in the *gtaG*⁻ mutant (*dstA* in Fig. 2C). Members of the 57-amino-acid

Journal of Cell Science (2016) 129, 1722-1733 doi:10.1242/jcs.181545

Table 1. Selected GO terms enriched in the list (induced or repressed) of GtaG-dependent genes

List_induced

GO.ID[a]	GO.Term[b]	Annotated[c]	Significant[d]	Expected[e]	*P*-value[f]	Enrichment[g]	Category[h]
GO:0030248	Cellulose binding	19	11	1.69	9.8×10^{-8}	6.5	MF
GO:0005200	Structural constituent of cytoskeleton	34	13	3.02	3.0×10^{-6}	4.3	MF
GO:0017022	Myosin binding	43	13	3.82	5.7×10^{-5}	3.4	MF
GO:0008810	Cellulase activity	7	4	0.62	1.7×10^{-3}	6.5	MF
GO:0006972	Hyperosmotic response	57	19	4.90	1.2×10^{-7}	3.9	BP
GO:0048869	Cellular developmental process	186	36	16.00	2.5×10^{-6}	2.3	BP
GO:0000902	Cell morphogenesis	48	13	4.13	1.4×10^{-4}	3.1	BP
GO:0043934	Sporulation	81	17	6.97	4.3×10^{-4}	2.4	BP
GO:0030154	Cell differentiation	142	24	12.22	9.6×10^{-4}	2.0	BP
GO:0030245	Cellulose catabolic process	7	4	0.6	1.5×10^{-3}	6.7	BP
GO:0044291	Cell-cell contact zone	23	13	1.94	5.1×10^{-9}	6.7	CC
GO:0005911	Cell-cell junction	32	15	2.71	9.7×10^{-9}	5.5	CC
GO:0005884	Actin filament	30	13	2.54	3.0×10^{-7}	5.1	CC
GO:0005576	Extracellular region	514	65	43.46	4.7×10^{-4}	1.5	CC

List_repressed

GO.ID	GO.Term	Annotated	Significant	Expected	*P*-value	Enrichment	Category
GO:0016655	Oxidoreductase activity, acting on NAD(P)H, quinone or similar compound as acceptor	28	14	4.91	8.4×10^{-5}	2.9	MF
GO:0004930	G-protein-coupled receptor activity	33	13	5.79	2.5×10^{-3}	2.2	MF
GO:0001056	RNA polymerase III activity	19	9	3.33	2.6×10^{-3}	2.7	MF
GO:0035493	SNARE complex assembly	6	6	1.07	3.2×10^{-5}	5.6	BP
GO:0045814	Negative regulation of gene expression, epigenetic	5	5	0.89	1.8×10^{-4}	5.6	BP
GO:0016458	Gene silencing	20	11	3.56	1.9×10^{-4}	3.1	BP
GO:0016575	Histone deacetylation	8	6	1.43	6.4×10^{-4}	4.2	BP
GO:1902275	Regulation of chromatin organization	8	6	1.43	6.4×10^{-4}	4.2	BP
GO:0006359	Regulation of transcription from RNA polymerase II promoter	4	4	0.71	1.0×10^{-3}	5.6	BP
GO:0042144	Vacuole fusion, non-autophagic	7	5	1.25	2.7×10^{-3}	4.0	BP
GO:0051028	mRNA transport	19	9	3.39	2.9×10^{-3}	2.7	BP
GO:0005763	Mitochondrial small ribosomal subunit	6	6	1.07	3.1×10^{-5}	5.6	CC
GO:0000439	Core TFIIH complex	5	5	0.89	1.8×10^{-4}	5.6	CC
GO:0030897	HOPS complex	7	5	1.24	2.7×10^{-3}	4.0	CC
GO:0005666	DNA-directed RNA polymerase III complex	19	9	3.37	2.9×10^{-3}	2.7	CC

[a]The unique GO-term identifier.
[b]Abbreviated description of the GO term.
[c]The number of genes in the genome with the indicated annotation.
[d]The number of genes in the gene set with the indicated annotation.
[e]The predicted number in the input list, based on the background frequency, which is the proportion of the annotated genes in the total annotated gene set.
[f]*P*-value <0.01 (Fisher's exact test).
[g]The ratio of 'Significant' to 'Expected'.
[h]The GO-term category (MF, molecular function; BP, biological process; CC, cellular component).

protein family are highly similar to each other, most of the genes encoding these proteins are located in a cluster on Chromosome 4 (Fig. S4) and the expression of some is also GbfA-dependent (Iranfar et al., 2006). Many genes of this family are highly expressed during development, and most of them are predominantly expressed in prestalk cells (Fig. S4C; Parikh et al., 2010). In the *gtaG*$^{-}$ mutant, *hssA* was underexpressed after 12 h of development (Fig. 2C), and some of the 57-amino-acid-family genes, including DDB_G0283421 and DDB_G0286193, exhibited similar expression patterns (Fig. S4D). The functions of these gene families are unknown, but their dependence on GtaG suggests a link between GtaG, GbfA and Dd-STATa.

Two of the interesting differentially expressed genes, *ecmF* and *dgcA*, were chosen for additional analysis from the induced-gene list (Fig. 2C; Table S2).

gtaG is required for *ecmF* expression

ecmF encodes a putative cellulose-binding extracellular matrix protein. It has been characterized as a cell-type-specific marker gene (Maeda et al., 2003) and a putative transcriptional target of Dd-

Journal of Cell Science (2016) 129, 1722-1733 doi:10.1242/jcs.181545

STATa, but its function is unknown because an *ecmF*-knockout mutation has no obvious phenotype (Shimada et al., 2004). Our RNA-seq data showed that *ecmF* mRNA accumulates during late development, peaking at 20 h in the wild type, whereas it was barely detectable in the *gtaG*$^{-}$ mutant (Fig. 3A). Furthermore, *ecmF* mRNA accumulates preferentially in PST-A cells (Maeda et al., 2003; Shimada et al., 2004), similar to *gtaG*, so it might be a direct target of the GtaG transcription factor activity. To test that possibility, we generated a reporter construct in which the *ecmF* promoter was fused to the *E. coli* β-galactosidase gene (*ecmF/lacZ*), and transformed it into *D. discoideum* cells. As a control, we chose *ecmA* because it did not exhibit differential expression between the wild type (AX4) and the *gtaG*$^{-}$ mutant in the RNA-seq data (Fig. 3A). In addition, the *ecmA/lacZ* reporter labels most of the prestalk cells (Early et al., 1993). We found that *ecmF/lacZ* activity in the wild type was specific to PST-A cells at the finger stage, and that it localized to the elongating stalk tube at early culmination and to the anterior part of the stalk at late culmination (Fig. 3B), nearly identical to the published RNA *in situ* hybridization pattern of *ecmF* expression (cDNA clone SLF308 in Maeda et al., 2003; Shimada et al., 2004). This finding suggests that the reporter construct faithfully represents the promoter activity. In the *gtaG*$^{-}$ background, *ecmF/lacZ* expression was undetectable by performing X-gal staining in *gtaG*$^{-}$ fingers. In rare cases, where aberrant culmination took place, we observed light staining at the very end of the tips (Fig. 3C), suggesting that GtaG is required for proper *ecmF* expression, especially in the elongating stalk tube and stalk cells at culmination. In the control experiments, we found no obvious difference between the wild type and the mutant regarding the spatial pattern of *ecmA/lacZ* expression (Fig. 3D,E) and *ecm0/lacZ* expression (Fig. 3F,G), suggesting that the *gtaG*$^{-}$ mutation does not have a wholesale effect on the function of prestalk cells, PST-A cells, PST-O cells and some of the ALCs. To quantify these findings, we measured the catalytic activity of β-galactosidase in the reporter strains. The results shown in Fig. 3J support the spatial information – *ecmF* expression is greatly dependent on *gtaG* whereas *ecmA* expression is independent. Moreover, we also examined the effect of GtaG function on PST-B cells. In the RNA-seq data, the PST-B marker gene *ecmB* was expressed normally until 16 h of development in the *gtaG*$^{-}$ mutant, but it was

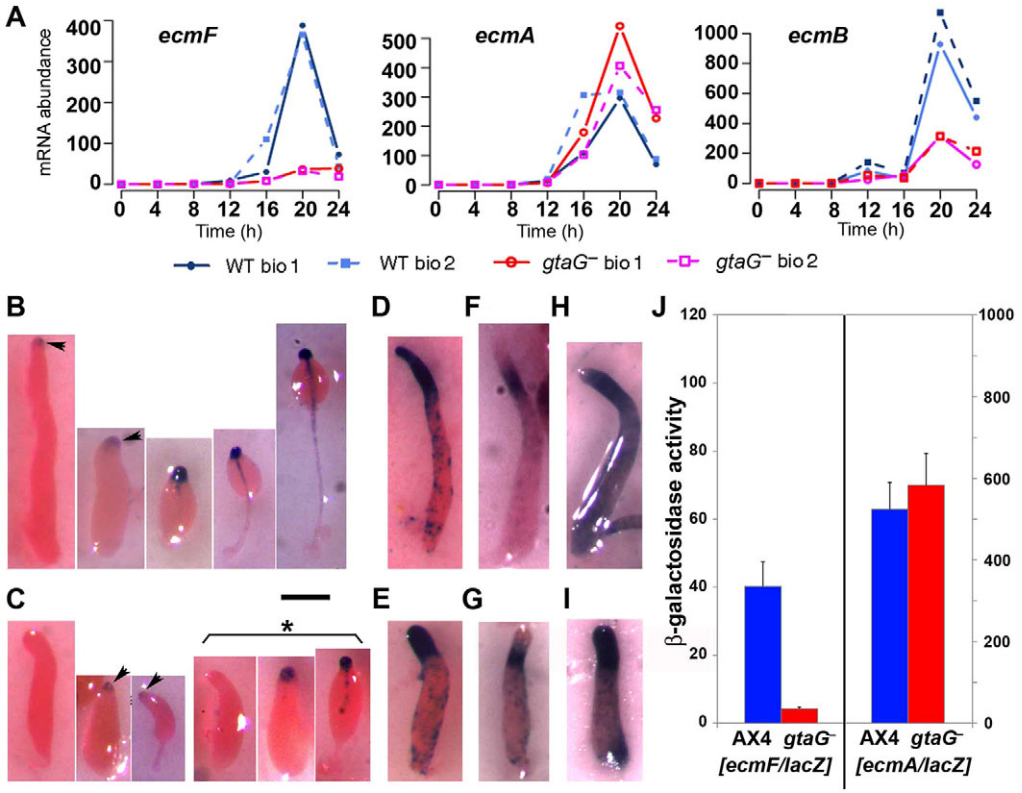

Fig. 3. The *gtaG*$^{-}$ gene is required for PST-A cell differentiation. (A) We obtained data from the RNA-seq experiments in Fig. 2 and plotted the standardized mRNA abundance (y-axis) of *ecmF* (left panel), *ecmA* (middle panel) and *ecmB* (right panel) in the wild type (WT; AX4, blue and light blue) and in the *gtaG*$^{-}$ mutant (red and magenta) as a function of developmental time (hours, x-axis). The solid and dotted lines represent two biological replications as indicated. (B–I) We used strains carrying the prestalk marker *ecmF/lacZ*, which labels PST-A cells, the prestalk marker *ecmA/lacZ*, which labels most of the prestalk cells, the PST-O marker *ecmO/lacZ*, or the PST-B marker *ecmB/lacZ*. We developed the cells on nitrocellulose filters to monitor β-galactosidase activity. We fixed developmental structures and stained them with X-gal. (B) Spatial expression of *ecmF/lacZ* in wild type (AX4) at the finger stage and in progressive stages of culmination (from left to right). Arrowheads indicate weak X-gal staining. (C) Spatial expression of *ecmF/lacZ* in mutant (*gtaG*$^{-}$) at the finger stage and in progressive stages of aberrant culmination. Arrowheads indicate weak X-gal staining in the later developing structures. An asterisk indicates the long-exposure images of *gtaG*$^{-}$ finger and culminant stages. (D) *ecmA/lacZ* in wild type (AX4); (E) *ecmA/lacZ* in mutant (*gtaG*$^{-}$) fingers. (F) *ecmO/lacZ* in wild type (AX4); (G) *ecmO/lacZ* in mutant (*gtaG*$^{-}$) fingers. (H) *ecmB/lacZ* in wild type (AX4); (I) *ecmB/lacZ* in mutant (*gtaG*$^{-}$) fingers. Scale bar: 0.2 mm. (J) We lysed the cells after 19 h of development and measured enzyme activity by performing the ONPG assay to compare promoter activity between the strains. Different y-axes are shown because the promoter strengths are vastly different. The left y-axis describes the *ecmF/lacZ* strain, and the right y-axis describes the *ecmA/lacZ* strain. In both cases, the wild type (AX4) is shown in blue and the mutant (*gtaG*$^{-}$) in red. The data are the means±s.e.m. of two independent clonal strains, each done in three independent replicates.

Journal of Cell Science (2016) 129, 1722-1733 doi:10.1242/jcs.181545

significantly underexpressed at later time points (Fig. 3A). X-gal staining fingers that were developing at 16 h also showed no obvious difference between the wild type and the mutant regarding the spatial pattern of *ecmB/lacZ* expression (Fig. 3H,I).

Some of the *gtaG*$^-$ phenotypes are non-cell-autonomous (Fig. 1), but if GtaG were indeed a direct regulator of *ecmF* expression, then the *ecmF* expression phenotype should be cell-autonomous. To test that possibility, we made chimerae in which *gtaG*$^-$ mutant cells carrying *ecmF*/*lacZ* were mixed with unlabeled AX4 or *gtaG*$^-$ mutant cells and measured the spatial pattern and level of β-galactosidase activity (Fig. 4). We found that the regulation of *ecmF*/*lacZ* activity by *gtaG* was cell-autonomous. The *gtaG*$^-$ mutant exhibited similar levels of X-gal staining in the PST-A region in either chimerae with unlabeled AX4 cells or unlabeled *gtaG*$^-$ mutant cells at 21 h of development (Fig. 4A,B), indicating that *ecmF* expression in the *gtaG*$^-$ mutant is unaffected by the neighboring wild-type cells. In the control chimerae between unlabeled *gtaG*$^-$ and labeled AX4 cells, AX4 cells exhibited strong X-gal staining in the PST-A region and in the descending stalk tube (Fig. 4C), indicating that the *ecmF* expression phenotype is indeed cell-autonomous. Further support for that conclusion is provided in Fig. 4D, where quantitative analysis of β-galactosidase activity in the three types of chimera shows that each chimera exhibited about half the activity of the respective pure populations, and that *gtaG*$^-$ cells carrying *ecmF*/*lacZ* expressed low levels of *ecmF*/*lacZ* regardless of the chimeric partner genotype (red bar graphs: '*gtaG*$^-$*[F/lacZ]*+AX4' and '*gtaG*$^-$*[F/lacZ]*+*gtaG*$^-$' in Fig. 4D). These results suggest that GtaG acts as a direct regulator of the *ecmF* promoter, but it is clear that other regulators are also involved because *ecmF* expression is not completely abolished in the absence of GtaG.

Relationships between *gtaG* and culmination-signaling molecules

dgcA encodes diguanylate cyclase, an enzyme that synthesizes c-di-GMP. The *dgcA* promoter is active in prestalk cells, and the phenotype of the *dgcA*$^-$ mutant is similar to that of the *gtaG*$^-$ mutant (Chen and Schaap, 2012). Because the differential expression analysis revealed that *dgcA* expression at 20 h of development was slightly but significantly reduced in the *gtaG*$^-$ mutant (Table S2), we wanted to test the functional relationship between the two genes, even though the expression pattern of *dgcA* (Chen and Schaap, 2012) suggests that *gtaG* is not a major regulator of *dgcA* expression throughout development. Testing the sporulation efficiency of the relevant mutants indicated that both *gtaG*$^-$ and *dgcA*$^-$ mutants were severely defective in sporulation when they developed in pure populations, and mixing experiments with the wild type showed that these defects are non-cell-autonomous, albeit to different extents (Figs 1D,E and 5A). Mixing the two mutants together did not alleviate the sporulation defects in either mutant, suggesting that the non-cell-autonomous sporulation defects of two mutants might have a common molecular basis because just the addition of c-di-GMP can restore *dgcA*$^-$ mutant deficiency (Chen and Schaap, 2012). The simplest explanation is that *gtaG*$^-$ cells fail to sporulate because they are defective in c-di-GMP production. To test that possibility, we added c-di-GMP to developing fingers of *gtaG*$^-$ cells and measured their ability to sporulate. Fig. 5B shows that addition of c-di-GMP at the finger stage restored *gtaG*$^-$ sporulation efficiency in a concentration-dependent manner, with 2 mM c-di-GMP resulting in sporulation levels that were indistinguishable from those of the wild type. Developmental morphogenesis was also rescued by c-di-GMP – we developed *gtaG*$^-$ cells to the finger stage (Fig. 5C)

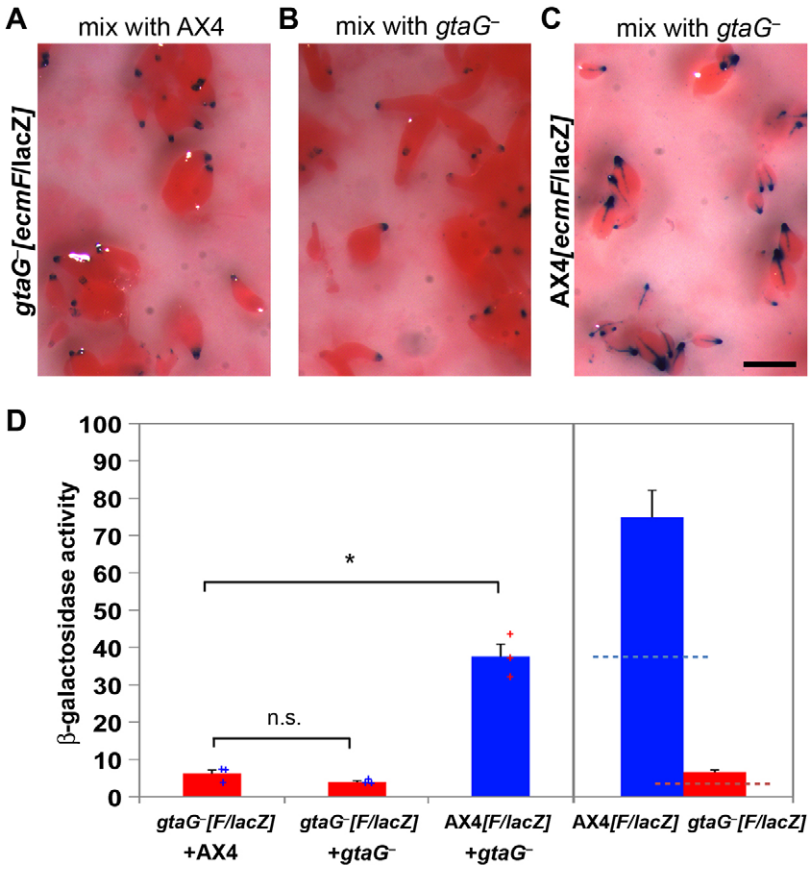

Fig. 4. The PST-A defect of *gtaG*$^-$ is cell-autonomous. We used wild-type and *gtaG*$^-$ strains, either unlabeled or labeled with the PST-A marker *ecmF*/lacZ, and made chimerae (1:1 ratio) of one labeled strain with one unlabeled strain. We developed the cells on nitrocellulose filters for 21 h and monitored β-galactosidase activity. We fixed whole-mount structures and stained them with X-gal. (A) Unlabeled wild type (AX4) mixed with *gtaG*$^-$ carrying *ecmF*/*lacZ*; (B) unlabeled *gtaG*$^-$ mutant mixed with *gtaG*$^-$ carrying *ecmF*/*lacZ*; (C) unlabeled *gtaG*$^-$ mutant mixed with wild type (AX4) carrying *ecmF*/*lacZ*. Scale bar: 0.5 mm. (D) We lysed the cells and measured enzyme activity by using the ONPG assay (y-axis) to compare different mixes as indicated on the x-axis (*F*, *ecmF*, left panel). Blue and red symbols (+) represent individual data points. The data are the means±s.e.m. of three independent replicates. Statistical analysis was conducted by performing paired two-tailed Student's *t*-test (n.s., not significant; *P<0.05). We also plotted the enzyme activity of 21-h developing cells in pure populations (right panel) and showed half the level of enzyme activity in the pure populations (colored dashed lines) to compare enzyme activities in a mixed population. The data are the means±s.e.m. of two independent clonal strains, each performed as three independent replicates.

Journal of Cell Science (2016) 129, 1722-1733 doi:10.1242/jcs.181545

and added buffer or 1 mM c-di-GMP. After 12 h, the buffer control sample was still at the finger stage (Fig. 5D), whereas many of the structures that had been treated with c-di-GMP developed into fruiting bodies (Fig. 5E). The restored fruiting bodies seemed to fall down easily, suggesting some other factor is required for proper stalk cell differentiation. These results suggest a causal relationship between GtaG activity, DgcA activity and c-di-GMP production.

The secreted peptides signals SDF-1 and SDF-2 are also components of the culmination-signaling pathway (Anjard et al., 1998a,b; Anjard et al., 2011; Anjard and Loomis, 2005). To study the GtaG pathway further, we tested the *gtaG*$^{-}$ cells in mixing experiments with *tagB*$^{-}$ cells, which cannot process the precursor of SDF-1, and *acbA*$^{-}$ cells, which cannot produce the precursor of SDF-2 (*tagB* and *acbA* expression are independent of GtaG) (Fig. 6A). Mixing of *gtaG*$^{-}$ cells with *acbA*$^{-}$ cells resulted in sporulation of both strains, whereas mixing of *gtaG*$^{-}$ cells with *tagB*$^{-}$ cells did not restore the sporulation of either strain (Fig. 6B). These results suggest that the *gtaG*$^{-}$ mutant strain is able to release SDF-2 but that its SDF-1 signaling pathway is compromised (Fig. 7). We also performed mixing experiments with *dstA*$^{-}$ cells, which is the Dd-STATa-null mutant. As expected, the *dstA*$^{-}$ strain did not synergize with the *gtaG*$^{-}$ strain (Fig. 6B), suggesting that GtaG and Dd-STATa have overlapping functions in terminal differentiation. This result is consistent with the fact that GtaG shares some of targets of Dd-STATa (Fig. 7).

DISCUSSION

The mutant phenotypes indicate that *gtaG* is essential for terminal differentiation in *D. discoideum*. Morphologically, the *gtaG*$^{-}$ mutant fails to progress beyond the finger stage of development, and fruiting body formation is greatly compromised. The molecular phenotypes, including RNA-seq and *ecmF/lacZ* reporter expression, support this conclusion and extend it by showing that most of the developmental transcriptional program is halted after the finger stage. The observations that spore formation is not completely abolished in the mutant and that *gtaG* is a prestalk-specific gene suggest that the *gtaG*$^{-}$ phenotype is cell-autonomous in prestalk cells and non-cell-autonomous in prespore cells. The mixing experiments confirmed that idea – the *ecmF* expression phenotype is cell-autonomous and the sporulation defect is not. Moreover, the inability of the *gtaG*$^{-}$ mutant to synergize with the *dgcA*$^{-}$ or *tagB*$^{-}$ mutants and the finding that adding exogenous c-di-GMP rescues *gtaG*$^{-}$ sporulation suggest that the sporulation defect in the *gtaG*$^{-}$ mutant is due to defective signaling from prestalk cells to prespore cells during culmination. The role of prestalk cells in signaling to prespore cells during culmination is well documented, because inactivation of prestalk cell differentiation by various means results in complete loss of sporulation that can be reversed by mixing with wild-type cells (Harwood et al., 1993; Shaulsky et al., 1995). Signaling is effected through an intricate system that coordinates culmination and terminal differentiation, involving secretion of the polyketide 4-methyl-5-pentylbenzene-1,3 diol (MPBD) that is produced by StlA and the small peptide SDF-1 that is processed by TagB (Anjard et al., 2011; Narita et al., 2011). In addition, c-di-GMP is a stalk-inducing morphogen that is also essential for spore formation in a non-cell-autonomous way, although the direct function of c-di-GMP in sporulation is unclear (Chen and Schaap, 2012). Our experiments cannot precisely

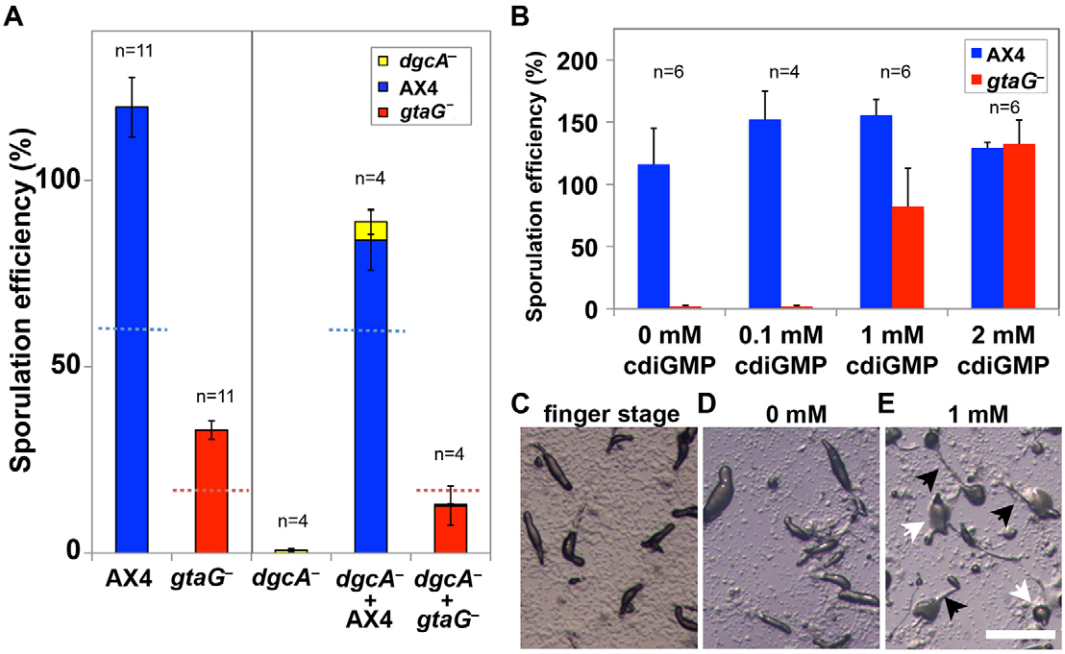

Fig. 5. c-di-GMP can rescue the culmination defect of *gtaG*$^{-}$. (A) We developed wild-type (AX4–DsRed, blue bars) and mutant cells (*gtaG*$^{-}$–GFP, red bars) in chimerae with unlabeled *dgcA*$^{-}$ cells (yellow bars), which are defective in c-di-GMP production. We compared the sporulation efficiencies (%, y-axis) of the three strains in pure populations and in chimerae, as indicated below the x-axis. The data are the means±s.e.m. of four independent replicates for the *dgcA* mixes. Dashed lines show half the level of sporulation efficiency in each pure population and the level expected in the absence of synergy in the mixed populations. (B) We developed wild-type (AX4, blue bars) and mutant (*gtaG*$^{-}$, red bars) cells on nitrocellulose filters for 16 h. We then added the indicated concentration of c-di-GMP on top of the fingers, incubated for 12 more hours and measured the sporulation efficiency (%, y-axis). The data are the means±s.e.m. of 4–6 independent replicates. We also developed *gtaG*$^{-}$ cells on agar plates until they reached the finger stage (C) and added buffer (D) or 1 mM c-di-GMP (E) on top of the fingers. We incubated the plates for 12 more hours and photographed the structures from above. White arrows indicate the later developing structures, and black arrows indicate stalks. Scale bar: 0.5 mm.

Journal of Cell Science (2016) 129, 1722-1733 doi:10.1242/jcs.181545

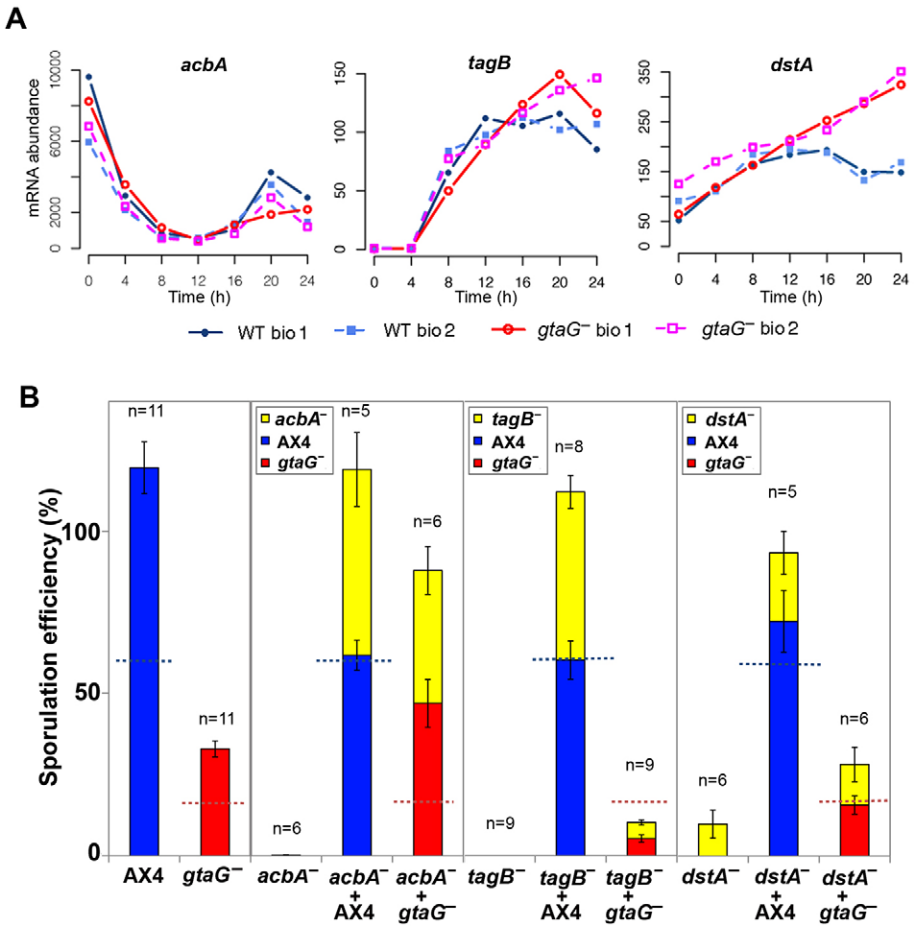

Fig. 6. Chimerae between *gtaG*⁻ cells and other developmental mutants. (A) We plotted the standardized mRNA abundance (y-axis) of the following genes as a function of developmental time (hours, x-axis): *acbA*, *tagB* and *dstA*, as indicated above each profile. Two biological replicates of the wild type (WT; AX4, blue solid line and dashed light blue line) and the *gtaG*⁻ mutant (red sold line and magenta dashed line) are shown in each graph. (B) We developed cells in pure populations or in chimerae as indicated on the x-axis and compared the sporulation efficiencies (%, y-axis). The genotypes are indicated by colors in each panel. The data are the means±s.e.m. of 5–11 independent replicates. Dashed lines show half the level of sporulation efficiency in each pure population and the level expected in the absence of synergy in the mixed populations.

determine which prestalk-to-prespore signal is compromised in the *gtaG*⁻ mutant, but they suggest that the c-di-GMP and SDF-1 signaling pathways are disrupted. These findings are consistent with the observation that expression of the c-di-GMP synthetic gene *dgcA* is compromised in the *gtaG*⁻ mutant. GtaG might regulate some other factors that control the proper amount or timing of c-di-GMP production. Our finding that addition of c-di-GMP largely rescued the *gtaG*⁻ culmination and sporulation defects despite the deficiency of SDF-1 signaling also raises a possibility of crosstalk between the c-di-GMP and SDF-1 signaling pathways. In addition, the fragility of the stalks in the fruiting bodies restored by c-di-GMP suggests that GtaG has both cell-autonomous and non-cell-autonomous functions in stalk differentiation.

We have not tested whether GtaG is indeed a transcription factor, but its sequence features and the mutant phenotype support that possibility, and there is no evidence against it. GtaG is likely to be one of the terminal nodes in a transcriptional regulatory network that functions in the specification and differentiation of prestalk cells. *gtaG* mRNA accumulates preferentially in PST-A cells, and the *gtaG* promoter is active almost exclusively in these cells, suggesting that it is subject to tight regulation in the PST-A region. GtaG does not seem to regulate its own expression because the *gtaG* promoter is active in the *gtaG*⁻ mutant, as indicated by the RNA-seq experiments. Therefore, at least one other transcription factor must be at play in specifying this expression pattern. Several lines of evidence suggest that Dd-STATa is involved. First, many Dd-STATa-dependent transcripts, including *ecmF*, *ecmJ* and *aslA* (Shimada et al., 2004), are *gtaG*-dependent. Second, *gtaG* is essential for the expression of several genetic suppressors of the Dd-STATa-defective phenotype (Shimada et al., 2008), including some members of the hssA/7E/2C family. Third, *dstA*⁻ cells fail to synergize with *gtaG*⁻ cells in mixing experiments. However, the relationship between GtaG and Dd-STATa might not be simple. Dd-STATa was overexpressed after 12 h of development in the *gtaG*⁻ mutant (Fig. 6A), but the Dd-STATa-dependent transcript *ecmF* is probably directly and positively regulated by GtaG. Another target gene, *ecmB*, is expressed normally in the *gtaG*⁻ fingers, even though Dd-STATa directly represses *ecmB* expression in PST-A cells (Mohanty et al., 1999). The precise gene-regulatory networks that control culmination are therefore not quite clear yet.

Some of the genes whose expression depends on *gtaG* and on Dd-STATa encode cellulose-binding proteins, and some of these proteins have been identified as extracellular matrix components of the slug sheath and the stalk (Wang et al., 2001). Interestingly, Loomis has proposed that culmination is caused by changes in sheath properties at the tip of the slug (Loomis, 2015). The specific expression of *gtaG* and its downstream genes (e.g. *ecmF*) at the tip of the slug suggests that *gtaG* could participate in terminal differentiation by regulating culmination through regulation of sheath properties.

MATERIALS AND METHODS

Cell culture, strain maintenance and development

We maintained *D. discoideum* cells at 22°C in HL5 liquid medium with the necessary supplements as indicated in Table S3. To induce development, we collected mid-log growing cells and washed them twice in 20 mM potassium phosphate buffer (KK2; pH 6.4) (Katoh et al., 2004). We deposited 1.8×10^6 cells/cm^2 on nitrocellulose filters on top of a PDF-buffer-

Journal of Cell Science (2016) 129, 1722-1733 doi:10.1242/jcs.181545

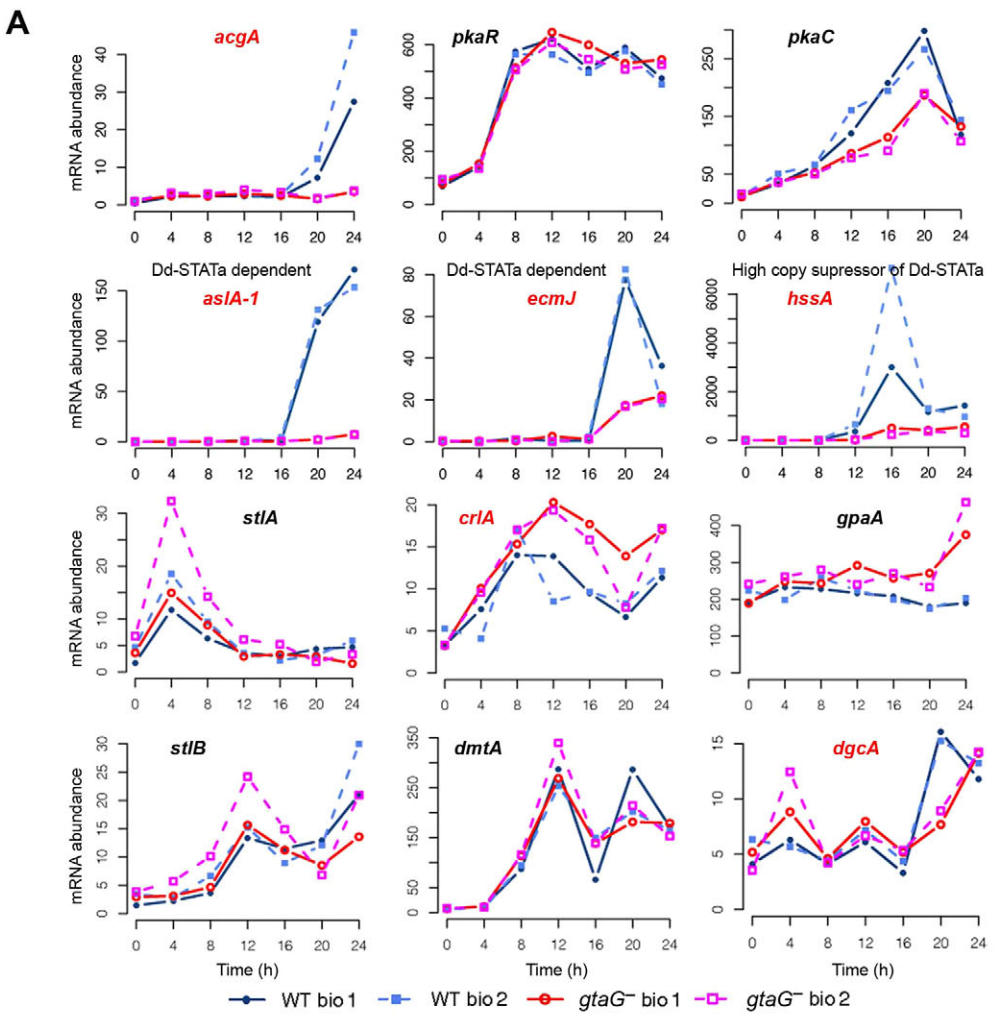

Fig. 7. Expression profiles of genes that are related to culmination. (A) We plotted the standardized mRNA abundance (y-axis) of the following genes as a function of developmental time (hours, x-axis): *acgA*, *pkaR*, *pkaC*, *aslA-1*, *ecmJ*, *hssA*, *stlA*, *crlA*, *gpaA*, *stlB*, *dmtA* and *dgcA*, as indicated above each profile. The gene names given in red are genes that exhibit significant differential expression between *gtaG*$^{-}$ and AX4. Two biological replicates of the wild type (WT; AX4, blue solid line and dashed light blue line) and the *gtaG*$^{-}$ mutant (red sold line and magenta dashed line) are shown in each graph. (B) A proposed model for the mode of action of GtaG and its relationships to other regulators of culmination and the transcriptional regulator Dd-STATa. SDF-1 production depends on *tagB*, which seems to be independent of GtaG, but SDF-1 leads to induction of *acgA* activity, and *acgA* expression is regulated by GtaG. GtaG is also likely to be a regulator of the c-di-GMP production gene *dgcA*. GtaG has a small effect on the expression of *pkaC* as well, but it is not the major regulator of this central gene. GtaG might partially regulate *crlA*, which is the membrane receptor of MPBD and is required to release SDF-1 (Anjard et al., 2011). However, the expression of *stlA* (polyketide synthase for MPBD), *stlB* (polyketide synthase to produce the backbone of DIF-1) and *dmtA* (methyltransferase to catalyze the last step in DIF-1 synthesis) is not affected by loss of *gtaG* function. Both GtaG and Dd-STATa regulate the expression of many cellulose-binding proteins, and GtaG might directly regulate the expression of Dd-STATa at some level from the late aggregation stage through the end of development.

soaked paper pad or KK2 agar plate and incubated them at 22°C for development. PDF buffer was composed of 20.1 mM KCl, 5.3 mM $MgCl_2$, 9.2 mM K_2HPO_4, 13.2 mM KH_2PO_4 and 1 mM $CaCl_2$.

Plasmid construction and mutant generation

We generated the *gtaG* insertion mutation by homologous recombination using the plasmid rescued from BCM REMI insertional mutant V10633 (Fig. S2; Sawai et al., 2007). To knock *gtaG* out, we first amplified the entire *gtaG* ORF by performing PCR using the following primer set: *kpn*I-gtaG_F: 5′-GGGGTACCATGAAATTATATTCTATTGACTTTCC-3′ and *kpn*I-gtaG_R: 5′-GGGGTACCATTTAAAGTATTTCTTGTATTTTCAGG-3′ and cloned the DNA fragment into pCR™-Blunt II-TOPO (Invitrogen). Then, we digested with *Mfe*I restriction endonuclease to delete the region between base pairs 785 and 2165 of the *gtaG* ORF and ligated with a BSR-cassette flanked by *Eco*RI sites (the plasmid was a kind gift from Chris Thompson, University of Manchester, Manchester, UK). We linearized the plasmid with *Kpn*I restriction endonuclease and transformed it into AX4 cells (Kuspa and Loomis, 1992; Adachi et al., 1994). We selected the transformants with 10 µg/ml Blasticidin S and verified the homologous recombination mutants by performing Southern blot analysis and by PCR across the homologous recombination junctions using genomic DNA from the cloned strains (Fig. S3).

To generate LacZ reporter constructs, we used the Gateway® cloning system (Life Technologies). We cloned the upstream region of *gtaG* from −753 to +36, and *ecmF* from −677 to +33 in the pENTR™ Directional TOPO vector and performed LR recombination with pPT134 (from

Journal of Cell Science

Journal of Cell Science (2016) 129, 1722-1733 doi:10.1242/jcs.181545

dictyBase). We transformed these plasmids (p*gtaG*/lacZ and p*ecmF*/lacZ), in addition to pEcmA-Gal (Early et al., 1993), pEcmO-Gal (Early et al., 1995) and pEcmB-Gal (Jermyn and Williams, 1991), into AX4 or *gtaG*$^{-}$ cells and selected for resistance to 10 µg/ml G418.

RNA-seq

We collected samples at 4-h intervals during development in two independent replicates, prepared total RNA using Trizol (Invitrogen) and performed poly(A) selection twice, as described previously (Huang et al., 2011). We prepared multiplexed cDNA libraries and performed RNA-seq using the Illumina sequencing platform as described previously (Miranda et al., 2013).

Transcriptome analyses

We mapped the resulting sequences to the *Dictyostelium* reference genome and obtained mRNA abundance values for each gene in the genome, as described previously (Miranda et al., 2013). The data were deposited in Gene Expression Omnibus (GEO; accession number, GSE70558). We visualized relative distances between the wild-type and *gtaG*$^{-}$ transcriptomes using classic multi-dimensional scaling (R-function cmdscale) (Santhanam et al., 2015). All biological replicates were very similar to one another (Spearman's correlation ≥0.968). We performed differential expression analyses, as described previously with minor modifications (Santhanam et al., 2015). Using custom R scripts (baySeq R package version 2.0.50), we compared the transcriptomes between wild-type and *gtaG*$^{-}$ strains at each developmental time point and considered genes with false discovery rates (FDR) lower than 0.01 and likelihoods greater than 0.9 as differentially expressed genes (Table S2). We visualized the standardized mRNA abundance of genes that were differentially expressed at any time point during development as a heat map (R function heatmap.2). For gene ontology enrichment analyses on all gene sets (up or down at each time point and potential activated or repressed genes), we used custom R scripts (R package 'topGO' version 2.14.0) using the GO annotation files for *D. discoideum* from dictyBase (http://dictybase.org/). We also calculated the fold change in enrichment for cell-type-enriched genes, hssA/2C/7E-family genes and 57-amino-acid-family genes, which are not annotated as gene ontology terms, in the same way as in the gene ontology enrichment analyses. Briefly, the fold enrichment was calculated as the sample frequency, which is the proportion of the defined genes (Significant) in the input list, and was compared to the background frequency, which is the proportion of the defined genes (Annotated) in the whole genome. We used the Fisher's exact test to obtain *P*-values.

Mixing experiments and flow cytometry

We performed mixing experiments, as described previously with minor modifications (Ostrowski et al., 2008). After collecting each strain, we adjusted each cell suspension to a density of 1×10^8 cells/ml in PDF buffer. We mixed two strains in equal proportions, deposited 1.8×10^6 cells/cm^2 on a nitrocellulose filter and incubated them at 22°C for development. After 48 h, we collected whole cells in detergent solutions (to eliminate amoebae that had not sporulated) and measured the proportion of fluorescent (GFP or DsRed) and non-fluorescent spores within each mix by using the Attune Acoustic Focusing Cytometer. We also counted the spores by hand by using phase microscopy and calculated total spore numbers in each sample.

ONPG assay

We harvested developing cells, washed them in Z buffer (60 mM Na_2HPO_4, 40 mM NaH_2PO_4, 10 mM KCl, 1 mM $MgSO_4$, pH 7.0) and lysed them in Z buffer containing 1% Triton X-100. After removal of cell debris by centrifugation, we measured and calculated β-galactosidase enzyme activity using the ONPG assay, as described previously (Dingermann et al., 1989). Briefly, we incubated 20 µl of the cell extract with 100 µl of ONPG solution (1.6 mg/ml ONPG, 22.9 mM β-mercaptoethanol in Z buffer) at room temperature, terminated the reaction by adding 80 µl of 1 M Na_2CO_3 and monitored enzyme activity by performing spectrophotometry at 420 nm. Units of β-galactosidase enzyme activity were standardized by measuring the protein abundance, the reaction time and *lacZ* copy number (as determined by performing quantitative PCR).

X-gal staining

We performed X-gal staining to visualize β-galactosidase activity in whole mounts, as described previously with minor modifications (Shaulsky and Loomis, 1993). We fixed developing cells with 4% paraformaldehyde in KK2 buffer for 10 min and then permeabilized them with 0.1% NP-40 in Z buffer for 20 min. After washing once with Z buffer, we added X-gal staining solution {5 mM $K_3[Fe(CN)_6]$, 5 mM $K_4[Fe(CN)_6]$, 1 mg/ml X-Gal in N,N-dimethylformamide in Z buffer}, waited for the blue color to develop, washed with Z buffer and counterstained with eosin Y.

Induction of sporulation with c-di-GMP

We spotted 10-µl droplets of cells at a density of 1×10^8 cells/ml on black nitrocellulose filters and incubated them at 22°C until the finger stage (16 h). We added 10-µl droplets of c-di-GMP on top of the multicellular structures and continued incubation for another 12 h (total 28 h). We collected spores by harvesting the entire filter, counted the spores with phase microscopy and calculated sporulation efficiency as the proportion (%) of cells that became spores. We also performed c-di-GMP addition experiments on KK2 agar plates and photographed the developing cells before addition and after 12 h of incubation with c-di-GMP.

Acknowledgements

We thank M. Toplak, J. Kokošar, M. Stajdohar and B. Zupan from the University of Ljubljana for assistance with the RNA-seq data management and computational support; J. M. Sederstrom for expert assistance with cytometry and cell sorting; and A. Kuspa for useful suggestions and discussions. We thank Christopher Thompson for providing a plasmid containing the BSR-cassette with added *Eco*RI sites. We are grateful to the Dicty stock center for maintaining and providing vectors and strains.

Competing interests

The authors declare no competing or financial interests.

Author contributions

M.K.-K. and G.S. conceived and designed the experiments. M.K.-K. performed the experiments and M.K.-K. and B.S. analyzed the data. M.K.-K. and G.S. prepared the manuscript and all authors contributed to the discussion.

Funding

This work was supported by grants from the National Institute of Child Health and Human Development – 'the *Dictyostelium* Functional Genomics Program Project Grant' [grant number P01 HD39691 (to G.S.)]; and by the Cytometry and Cell Sorting Core at Baylor College of Medicine with funding from the National Institutes of Health [grant numbers P30 AI036211, P30 CA125123 and S10 RR024574]. Deposited in PMC for release after 12 months.

Data availability

The relevant data sets have been deposited under the accession number GSE70558 and can be accessed at http://www.ncbi.nlm.nih.gov/geo/query/acc.cgi?acc=GSE70558.

Supplementary information

Supplementary information available online at http://jcs.biologists.org/lookup/suppl/doi:10.1242/jcs.181545/-/DC1

References

Adachi, H., Hasebe, T., Yoshinaga, K., Ohta, T. and Sutoh, K. (1994). Isolation of *Dictyostelium discoideum* cytokinesis mutants by restriction enzyme-mediated integration of the blasticidin S resistance marker. *Biochem. Biophys. Res. Commun.* **205**, 1808-1814.

Anjard, C. and Loomis, W. F. (2005). Peptide signaling during terminal differentiation of *Dictyostelium*. *Proc. Natl. Acad. Sci. USA* **102**, 7607-7611.

Anjard, C., Su, Y. and Loomis, W. F. (2011). The polyketide MPBD initiates the SDF-1 signaling cascade that coordinates terminal differentiation in *Dictyostelium*. *Eukaryot. Cell* **10**, 956-963.

Anjard, C., Zeng, C., Loomis, W. F. and Nellen, W. (1998a). Signal transduction pathways leading to spore differentiation in *Dictyostelium discoideum*. *Dev. Biol.* **193**, 146-155.

Anjard, C., Chang, W. T., Gross, J. and Nellen, W. (1998b). Production and activity of spore differentiation factors (SDFs) in *Dictyostelium*. *Development* **125**, 4067-4075.

Basu, S., Fey, P., Jimenez-Morales, D., Dodson, R. J. and Chisholm, R. L. (2015). dictyBase 2015: Expanding data and annotations in a new software environment. *Genesis* **53**, 523-34.

Cai, H., Katoh-Kurasawa, M., Muramoto, T., Santhanam, B., Long, Y., Li, L., Ueda, M., Iglesias, P. A., Shaulsky, G. and Devreotes, P. N. (2014). Nucleocytoplasmic shuttling of a GATA transcription factor functions as a development timer. *Science* **343**, 1249531.
Chang, W.-T., Newell, P. C. and Gross, J. D. (1996). Identification of the cell fate gene stalky in *Dictyostelium*. *Cell* **87**, 471-481.
Chen, Z.-h. and Schaap, P. (2012). The prokaryote messenger c-di-GMP triggers stalk cell differentiation in *Dictyostelium*. *Nature* **488**, 680-683.
Dingermann, T., Reindl, N., Werner, H., Hildebrandt, M., Nellen, W., Harwood, A., Williams, J. and Nerke, K. (1989). Optimization and in situ detection of Escherichia coli beta-galactosidase gene expression in *Dictyostelium discoideum*. *Gene* **85**, 353-362.
Early, A. E., Gaskell, M. J., Traynor, D. and Williams, J. G. (1993). Two distinct populations of prestalk cells within the tip of the migratory *Dictyostelium* slug with differing fates at culmination. *Development* **118**, 353-362.
Early, A., Abe, T. and Williams, J. (1995). Evidence for positional differentiation of prestalk cells and for a morphogenetic gradient in *Dictyostelium*. *Cell* **83**, 91-99.
Eichinger, L., Pachebat, J. A., Glöckner, G., Rajandream, M.-A., Sucgang, R., Berriman, M., Song, J., Olsen, R., Szafranski, K., Xu, Q. et al. (2005). The genome of the social amoeba *Dictyostelium discoideum*. *Nature* **435**, 43-57.
Escalante, R. and Sastre, L. (1998). A Serum Response Factor homolog is required for spore differentiation in *Dictyostelium*. *Development* **125**, 3801-3808.
Fukuzawa, M., Hopper, N. and Williams, J. (1997). *cudA*: a *Dictyostelium* gene with pleiotropic effects on cellular differentiation and slug behaviour. *Development* **124**, 2719-2728.
Harwood, A. J., Early, A. and Williams, J. G. (1993). A repressor controls the timing and spatial localisation of stalk cell-specific gene expression in *Dictyostelium*. *Development* **118**, 1041-1048.
Huang, E., Blagg, S. L., Keller, T., Katoh, M., Shaulsky, G. and Thompson, C. R. L. (2006). bZIP transcription factor interactions regulate DIF responses in *Dictyostelium*. *Development* **133**, 449-458.
Huang, E., Talukder, S., Hughes, T. R., Curk, T., Zupan, B., Shaulsky, G. and Katoh-Kurasawa, M. (2011). BzpF is a CREB-like transcription factor that regulates spore maturation and stability in *Dictyostelium*. *Dev. Biol.* **358**, 137-146.
Iranfar, N., Fuller, D. and Loomis, W. F. (2006). Transcriptional regulation of post-aggregation genes in *Dictyostelium* by a feed-forward loop involving GBF and LagC. *Dev. Biol.* **290**, 460-469.
Jermyn, K. A. and Williams, J. G. (1991). An analysis of culmination in *Dictyostelium* using prestalk and stalk-specific cell autonomous markers. *Development* **111**, 779-787.
Katoh, M., Shaw, C., Xu, Q., Van Driessche, N., Morio, T., Kuwayama, H., Obara, S., Urushihara, H., Tanaka, Y. and Shaulsky, G. (2004). An orderly retreat: Dedifferentiation is a regulated process. *Proc. Natl. Acad. Sci. USA* **101**, 7005-7010.
Keller, T. and Thompson, C. R. (2008). Cell type specificity of a diffusible inducer is determined by a GATA family transcription factor. *Development* **135**, 1635-1645.
Kessin, R. H. (2001). *Dictyostelium: Evolution, Cell Biology, and the Development of Multicellularity*. Cambridge: Cambridge University Press.
Kessin, R. H. (2010). Two different genomes that produce the same result. *Genome Biol.* **11**, 114.
Kuspa, A. and Loomis, W. F. (1992). Tagging developmental genes in *Dictyostelium* by restriction enzyme-mediated integration of plasmid DNA. *Proc. Natl. Acad. Sci. USA* **89**, 8803-8807.
Loomis, W. F. (2015). Genetic control of morphogenesis in *Dictyostelium*. *Dev. Biol.* **402**, 146-161.
Lowry, J. A. and Atchley, W. R. (2000). Molecular evolution of the GATA family of transcription factors: conservation within the DNA-binding domain. *J. Mol. Evol.* **50**, 103-115.
Maeda, M., Sakamoto, H., Iranfar, N., Fuller, D., Maruo, T., Ogihara, S., Morio, T., Urushihara, H., Tanaka, Y. and Loomis, W. F. (2003). Changing patterns of gene expression in *Dictyostelium* prestalk cell subtypes recognized by in situ hybridization with genes from microarray analyses. *Eukaryot. Cell* **2**, 627-637.
Miranda, E. R., Rot, G., Toplak, M., Santhanam, B., Curk, T., Shaulsky, G. and Zupan, B. (2013). Transcriptional profiling of *Dictyostelium* with RNA sequencing. *Methods Mol. Biol.* **983**, 139-171.
Mohanty, S., Jermyn, K. A., Early, A., Kawata, T., Aubry, L., Ceccarelli, A., Schaap, P., Williams, J. G. and Firtel, R. A. (1999). Evidence that the *Dictyostelium* Dd-STATa protein is a repressor that regulates commitment to stalk cell differentiation and is also required for efficient chemotaxis. *Development* **126**, 3391-3405.
Mu, X., Spanos, S. A., Shiloach, J. and Kimmel, A. (2001). CRTF is a novel transcription factor that regulates multiple stages of *Dictyostelium* development. *Development* **128**, 2569-2579.
Narita, T. B., Koide, K., Morita, N. and Saito, T. (2011). *Dictyostelium* hybrid polyketide synthase, SteelyA, produces 4-methyl-5-pentylbenzene-1,3-diol and induces spore maturation. *FEMS Microbiol. Lett.* **319**, 82-87.
Ostrowski, E. A., Katoh, M., Shaulsky, G., Queller, D. C. and Strassmann, J. E. (2008). Kin discrimination increases with genetic distance in a social amoeba. *PLoS Biol.* **6**, e287.
Parikh, A., Miranda, E. R., Katoh-Kurasawa, M., Fuller, D., Rot, G., Zagar, L., Curk, T., Sucgang, R., Chen, R., Zupan, B. et al. (2010). Conserved developmental transcriptomes in evolutionarily divergent species. *Genome Biol.* **11**, R35.
Rosengarten, R. D., Santhanam, B. and Katoh-Kurasawa, M. (2013). Transcriptional regulators: dynamic drivers of multicellular formation, cell differentiation and development. In *Dictyostelids –Evolution, Genomics and Cell Biology* (ed. M. Romeralo, S. Baldauf and R. Escalante), pp. 89-108. Verlag Berlin Heidelberg: Springer.
Rosengarten, R. D., Santhanam, B., Fuller, D., Katoh-Kurasawa, M., Loomis, W. F., Zupan, B. and Shaulsky, G. (2015). Leaps and lulls in the developmental transcriptome of *Dictyostelium discoideum*. *BMC Genomics* **16**, 241.
Santhanam, B., Cai, H., Devreotes, P. N., Shaulsky, G. and Katoh-Kurasawa, M. (2015). The GATA transcription factor GtaC regulates early developmental gene expression dynamics in *Dictyostelium*. *Nat. Commun.* **6**, 7551.
Sawai, S., Guan, X.-J., Kuspa, A. and Cox, E. C. (2007). High-throughput analysis of spatio-temporal dynamics in *Dictyostelium*. *Genome Biol.* **8**, R144.
Schnitzler, G. R., Fischer, W. H. and Firtel, R. A. (1994). Cloning and characterization of the G-box binding factor, an essential component of the developmental switch between early and late development in *Dictyostelium*. *Genes Dev.* **8**, 502-514.
Shaulsky, G. and Huang, E. (2005). Components of the *Dictyostelium* gene expression regulatory machinery. In *Dictyostelium Genomics* (ed. W. F. Loomis and A. Kuspa), pp. 83-101. Norwich: Horizon Scientific Press.
Shaulsky, G. and Loomis, W. F. (1993). Cell type regulation in response to expression of ricin A in *Dictyostelium*. *Dev. Biol.* **160**, 85-98.
Shaulsky, G., Kuspa, A. and Loomis, W. F. (1995). A multidrug resistance transporter/serine protease gene is required for prestalk specialization in *Dictyostelium*. *Genes Dev.* **9**, 1111-1122.
Shimada, N., Nishio, K., Maeda, M., Urushihara, H. and Kawata, T. (2004). Extracellular matrix family proteins that are potential targets of Dd-STATa in *Dictyostelium discoideum*. *J. Plant Res.* **117**, 345-353.
Shimada, N., Kanno-Tanabe, N., Minemura, K. and Kawata, T. (2008). GBF-dependent family genes morphologically suppress the partially active *Dictyostelium* STATa strain. *Dev. Genes Evol.* **218**, 55-68.
Sucgang, R., Kuo, A., Tian, X., Salerno, W., Parikh, A., Feasley, C. L., Dalin, E., Tu, H., Huang, E., Barry, K. et al. (2011). Comparative genomics of the social amoebae *Dictyostelium discoideum* and *Dictyostelium purpureum*. *Genome Biol.* **12**, R20.
Teakle, G. R. and Gilmartin, P. M. (1998). Two forms of type IV zinc-finger motif and their kingdom-specific distribution between the flora, fauna and fungi. *Trends Biochem. Sci.* **23**, 100-102.
Thompson, C. R. L., Fu, Q., Buhay, C., Kay, R. R. and Shaulsky, G. (2004). A bZIP/bRLZ transcription factor required for DIF signaling in *Dictyostelium*. *Development* **131**, 513-523.
Van Driessche, N., Shaw, C., Katoh, M., Morio, T., Sucgang, R., Ibarra, M., Kuwayama, H., Saito, T., Urushihara, H., Maeda, M. et al. (2002). A transcriptional profile of multicellular development in *Dictyostelium discoideum*. *Development* **129**, 1543-1552.
Wang, Y., Slade, M. B., Gooley, A. A., Atwell, B. J. and Williams, K. L. (2001). Cellulose-binding modules from extracellular matrix proteins of *Dictyostelium discoideum* stalk and sheath. *Eur. J. Biochem.* **268**, 4334-4345.